J Therm Anal Calorim (2010) 101:455–461
DOI 10.1007/s10973-010-0790-0

Review of the thermodynamic and transport properties of $EuBr_2$–RbBr binary system

Leszek Rycerz · Ewa Ingier-Stocka ·
Slobodan Gadzuric · Marcelle Gaune-Escard

CCTA10 Special Issue

Abstract Differential Scanning Calorimetry was used to study phase equilibrium in $EuBr_2$–RbBr binary system. It was established that this system includes two eutectics and three stoichiometric compounds. First of them, Rb_2EuBr_4, decomposes peritectically at 778 K. Second one, $RbEuBr_3$, undergoes the solid–solid phase transition at 732 K and melts incongruently at 852 K. Third compound, $RbEu_2Br_5$, melts congruently at 888 K. The composition and temperature values of eutectics were determined as $x(EuBr_2) = 0.316$; $T_{eut} = 776$ K and $x(EuBr_2) = 0.797$; $T_{eut} = 859$ K. Mixing enthalpy was measured by direct calorimetry on the whole composition range. The minimum of the mixing enthalpy occurs around the composition $x(EuBr_2) \approx 0.4$. The electrical conductivity of liquid mixtures was also investigated over the whole composition range and measured down to temperatures below solidification. The specific conductance (liquid phase) plotted against the mole fraction of $EuBr_2$ shows a broad minimum at $x(EuBr_2) \sim 0.6$. The activation energy for conductivity changes with temperature. Results obtained are discussed in terms of possible complex formation.

Keywords Europium(II) bromide · Phase diagram · Electrical conductivity · Mixing enthalpy

Introduction

The lanthanides adopt predominantly the +3 oxidation state both in solution and in the solid state. However, there are some exceptions when lanthanides form stable compounds with the oxidation state +4 or +2. The oxidation state +2 is the predominant of europium. Indeed, the compounds of Eu(II) are more stable than those of Eu(III). Until now, only a very few studies have been carried out on divalent lanthanide-based melts. Experimental investigations were conducted very recently on $EuBr_2$ to assess the reliability of estimated temperature and enthalpy of fusion [1–4], entropy at 298 K, and the formation enthalpy of solid $EuBr_2$ at 298 K as well as the heat capacities of solid and liquid europium(II) bromide [5]. In view of the importance of $EuBr_2$ in many applications, e.g., the perspective storage X-ray phosphors for visualization of the X-ray images or luminophore plate production [6–8], we have initiated a research program focused both on $EuBr_2$ and its mixtures with alkali bromides. Previously, the thermodynamic and transport properties of $EuBr_2$ and $EuBr_2$-based binary mixtures with LiBr, NaBr, and KBr [9–12] were determined. Preliminary investigations were carried out on phase equilibria that existed in $EuBr_2$–RbBr binary system using differential scanning calorimetry method [13]. They revealed that three stoichiometric compounds are formed in this system, namely Rb_2EuBr_4, $RbEu_2Br_5$, and $RbEuBr_3$. The temperatures and enthalpies of phase transitions as well as the heat capacity dependence on temperature were determined for both solid and liquid Rb_2EuBr_4, $RbEu_2Br_5$, and solid $RbEuBr_3$ compounds, and

L. Rycerz · E. Ingier-Stocka (✉)
Faculty of Chemistry, Chemical Metallurgy Group, Wroclaw University of Technology, Wybrzeze Wyspianskiego 27, 50-370 Wroclaw, Poland
e-mail: ewa.ingier-stocka@pwr.wroc.pl

S. Gadzuric
Faculty of Natural Science, Department of Chemistry, University of Novi Sad, Trg. D. Obradovica 3, 21000 Novi Sad, Serbia

M. Gaune-Escard
Mecanique Energetique, Technopole de Chateau-Gombert, Ecole Polytechnique, 5 rue Enrico Fermi, 13453 Marseille Cedex 13, France

the results were presented in [14]. A polynomial heat capacity dependence on temperature

$$C^{0}_{\mathrm{pm}}/\mathrm{J\,mol^{-1}\,K^{-1}} = A + B \cdot (T/\mathrm{K}) + C \cdot (T/\mathrm{K})^{2} \qquad (1)$$

was used to fit the experimental data. The combination of these results with the entropy at 298.15 K, and the enthalpies of phase transitions enabled us to calculate the thermodynamic functions up to $T = 1100$ K.

The electrical conductivity measurements on $EuBr_2$–RbBr liquid mixtures were reported in our earlier article [15]. The studies were performed over the entire composition range (in steps of *ca.* 10 mol.%) of the binary system. It was established that the specific conductivity, κ, of each mixture showed some deviation from linearity when plotted against temperature as $\ln(\kappa) = f(1/T)$. Such a deviation from the classical Arrhenius equation was already mentioned in the literature [16], and observed by us also for several other lanthanide halide–alkali metal halide binary systems [15, 17–21]. For all of the investigated compositions, A_i coefficients were determined to fit experimental conductivity data equations:

$$\ln(\kappa) = A_0 + A_1 \cdot 10^3 \cdot \left(\frac{1}{T}\right) + A_2 \cdot 10^6 \cdot \left(\frac{1}{T}\right)^2 \qquad (2)$$

$$E_\mathrm{A} = -R\left[A_1 + 2A_2\left(\frac{1}{T}\right)\right] \qquad (3)$$

The above coefficients together with E_A values calculated at 1050 K were presented [15]. It was shown that the global relative conductivity changes are significantly larger in the rubidium bromide-rich region**.** We noticed a similar behavior in many other lanthanide halide–alkali metal halide binary systems [19–23]. Probably, when added to the ionic RbBr melt, $EuBr_2$ changes the coordination around rubidium ions while, conversely, the local arrangement around europium ions in pure $EuBr_2$ varies due to introduction of RbBr. In both cases, ionic conductivity decreases, and a broad minimum appears at $x(EuBr_2) \sim 0.6$. Unfortunately, no information regarding the structure of $EuBr_2$-based melts was found in the literature. However, analysis of the literature data on many alkali chloride–divalent metal chloride systems [24–26] indicate the existence of tetrahedral MCl_4^{2-} complexes. Moreover, it was proved experimentally that the structure of these melts depends on their composition [27, 28]. In addition, neutron diffraction experiments performed on the NaCl–$EuCl_2$ system [29] hint at the existence of tetrahedral $EuCl_4^{2-}$ complexes. The above mentioned facts suggest possibility of the existence of similar complexes, i.e., $EuBr_4^{2-}$ tetrahedral complex species, in $EuBr_2$-based melts. The increase of $EuBr_2$ M fraction in the melt leads to formation of polymeric forms of $EuBr_4^{2-}$. The observed dependence of activation energy (at 1050 K) on composition [15] validates the earlier statement made by Yaffe and van Artsdalen [30, 31] about the correlation between activation energy and structural changes in melts.

This study reports our recent results on europium(II) bromide–rubidium bromide binary system, i.e., the complete phase diagram and the determined mixing enthalpy values of the liquid mixtures over the entire composition range.

Experimental

Sample preparation

Europium(II) bromide was synthesised from the oxide Eu_2O_3 (Aldrich 99.9%) by a modified Haschke and Eick method [32]. The main steps of the synthesis included: dissolution of Eu_2O_3 in hot concentrated HBr acid, crystallization of $EuBr_3\bullet 6H_2O$, dehydration of hexahydrate, and thermal decomposition of $EuBr_3$ under reduced pressure. Chemical analysis of $EuBr_2$ obtained in this way was performed by mercurimetric (bromine) and complexometric (europium) methods. Europium and bromine content (Eu 48.74; 48.75% theoretical; Br 51.26; 51.25% theoretical) indicate the correctness of the method used.

Rubidium bromide was Merck Suprapur reagent (min. 99.9%). Prior to use, it was progressively heated up to fusion under gaseous HBr atmosphere. HBr in excess was then removed from the melt by argon bubbling.

The samples of the $EuBr_2$ and RbBr mixtures with the desired compositions were prepared in the procedure described later, beginning with the weighing of the appropriate portions of both components (see Table 1). All the mixtures were prepared in a glove box filled with purified and water-free argon. The prepared mixtures were melted in vacuum-sealed quartz ampoules in an electric furnace. The melts were homogenised by shaking and then solidified. Then, every sample was grounded in an agate mortar, and the homogenous sample of 300–500 mg was located in a DSC quartz ampoule (about 6-mm diameter; 15-mm length). All the above mentioned operations were done in a glove box. The ampoules filled with mixtures of different compositions (Table 1 and 2) were sealed under a reduced pressure of argon. The samples prepared along the same procedure were used in phase diagram measurements.

Measurements

The temperatures and enthalpies of phase transitions were measured with a Setaram DSC 121 differential scanning calorimeter. The apparatus and the measurements procedure were described in detail previously [33–35].

Table 1 Compositions of molten mixtures $EuBr_2$–RbBr used in DSC measurements

Sample no.	$m(EuBr_2)$/g	$m(RbBr)$/g	$x(EuBr_2)$
1	0.0516	0.5262	0.049
2	0.1044	0.5137	0.097
3	0.1733	0.5146	0.151
4	0.1383	0.2968	0.198
5	0.2617	0.4153	0.250
6	0.2051	0.2658	0.290
7	0.3167	0.3856	0.303
8	0.3367	0.3831	0.318
9	0.3442	0.3697	0.331
10	0.3789	0.3579	0.360
11	0.2865	0.2453	0.382
12	0.4402	0.3142	0.426
13	0.3427	0.1943	0.483
14	0.4256	0.2257	0.500
15	0.5281	0.2757	0.504
16	0.5521	0.2617	0.528
17	0.5770	0.2449	0.555
18	0.4252	0.1670	0.575
19	0.6229	0.2194	0.601
20	0.6748	0.1946	0.648
21	0.6913	0.1852	0.664
22	0.7318	0.1713	0.694
23	0.4922	0.1097	0.704
24	0.7607	0.1497	0.729
25	0.7819	0.1383	0.750
26	0.5528	0.0802	0.785
27	0.9223	0.1015	0.828
28	0.6170	0.0438	0.882
29	2.9402	0.1166	0.930

Enthalpies of transition measurements were conducted at heating and cooling rates in the range of 1–5 K min^{-1}.

The enthalpy-of-mixing experiments were all of the simple liquid–liquid type, performed under argon at atmospheric pressure. The calorimetric apparatus, a Calvet-type high-temperature microcalorimeter, the mixing devices used, and the experimental methods adopted have all been described in detail previously [34–36]. Europium(II) bromide was weighed in the glove box within 10^{-5} g and placed in the "break-off" quartz ampoule. The rubidium bromide, weighed in the same conditions, was placed in a quartz crucible. The break-off ampoule was evacuated under controlled argon pressure to obtain a pressure of 1 atm at the temperature of experiment. It was then welded to a quartz tube, which could be moved up and down the calorimetric cell through a special gastight ring.

The calorimetric cell was filled with argon and introduced in a Calvet calorimeter together with a reference cell. After thermal stabilization of the system, the ampoule was broken off against the inner break-off tip at the bottom of the quartz crucible, and thermal effect resulting from mixing was recorded. Calibration of the calorimeter was performed with α-alumina obtained from NIST. After the mixing experiments, pieces of α-alumina (30–100) mg were dropped into the melt, and the corresponding enthalpy increment was measured.

Results

$EuBr_2$–RbBr phase diagram

The $EuBr_2$–RbBr complete phase diagram was established for the first time in this study. DSC investigations performed on samples with different compositions (Table 1) yielded both the temperatures and enthalpy changes of the concerned mixtures. Owing to supercooling effect, all the temperature and enthalpy values reported in this study were determined from heating curves. The results are presented in Table 2.

In all the DSC curves, the effect at the highest temperature corresponds to liquidus. In the composition range $0 < x < 0.333$, where x is molar fraction of $EuBr_2$, one additional endothermic peak was present in all the heating DSC curves at 776 K (mean value for samples of different compositions—Table 2). Its disappearance at $x = 0.333$ suggests the existence of Rb_2EuBr_4 compound in the system under investigation. Thus, it can be undoubtedly ascribed to the RbBr–Rb_2EuBr_4 eutectic. The eutectic composition was determined accurately from the Tamman plot (Fig. 1a). The analysis of this experimental enthalpy versus composition plot evidences that no solid solutions are formed in the system. Thus, the corresponding straight lines intercept the composition axis at $x = 0$ and $x = 0.333$. The eutectic composition ($x = 0.316$) was determined from the intercept of the two linear parts in Fig. 1a. The eutectic temperature determined from all the appropriate DSC curves was found to be 776 K, whereas the enthalpy of fusion at the eutectic composition was equal 16.2 kJ mol^{-1}.

In general, three or four endothermic peaks in addition to liquidus were observed on heating curves for the samples with molar fraction of $EuBr_2$, $0.333 < x < 0.666$ (Tab.2). One of them at 778 K disappears for samples with $x \geq 0.500$, thereby suggesting the existence of $RbEuBr_3$ compound. Plot of enthalpy related to this effect versus composition (Fig. 1b) confirms the above postulated existence of Rb_2EuBr_4 compound. Accordingly, effect at 778 K results from incongruent melting of Rb_2EuBr_4. In

Table 2 DSC results for $EuBr_2$–RbBr binary system

Sample no.	$x(EuBr_2)$	T/K RbBr–Rb_2EuBr_4 eutectic	T/K Rb_2EuBr_4 decomposition	T/K $RbEuBr_3$ formation	T/K $RbEuBr_3$ transition	T/K $RbEuBr_3$ decomposition	T/K $RbEu_2Br_5$–$EuBr_2$ eutectic	T/K liquidus
1	0.000	–	–	–	–	–	–	967
2	0.049	773	–	–	–	–	–	948
3	0.097	775	–	–	–	–	–	923
4	0.151	775	–	–	–	–	–	882
5	0.198	778	–	–	–	–	–	853
6	0.250	778	–	–	–	–	–	818
7	0.290	780	–	–	–	–	–	785
8	0.303	781	–	–	–	–	–	787
9	0.318	779	–	–	–	–	–	776
10	0.331	–	778	–	–	–	–	778
11	0.360	–	778	634	732	–	–	806
12	0.382	–	780	635	733	–	–	833
13	0.426	–	776	632	727	–	–	852
14	0.483	–	778	633	733	852		860
15	0.500	–	779	631	730	855	–	855
16	0.504	–	–	631	727	853	–	862
17	0.528	–	–	629	727	856	–	867
18	0.555	–	–	638	730	850	–	872
19	0.575	–	–	635	733	851	–	866
20	0.601	–	–	635	732	853	–	879
21	0.648	–	–	–	731	850	–	887
22	0.664	–	–	–	–	–	–	888
23	0.694	–	–	–	–	–	857	883
24	0.704	–	–	–	–	–	860	882
25	0.729	–	–	–	–	–	857	880
26	0.750	–	–	–	–	–	859	875
27	0.785	–	–	–	–	–	859	869
28	0.828	–	–	–	–	–	860	866
29	0.882	–	–	–	–	–	859	894
30	0.930	–	–	–	–	–	858	918
31	1.000		–	–	–	–	–	935

addition, three endothermic effects were observed at 633, 732 and 852 K. Plot of enthalpy related to these effects versus composition (Fig. 1c, d and e) indicates undoubtedly that they are related to $RbEuBr_3$ compound. First of them at 852 K corresponds to incongruent melting of $RbEuBr_3$. The compound composition, $x = 0.516$ determined from the intercept of two straight lines in this Fig. 1e is in a good agreement with the theoretical value of $x = 0.500$. Similar Tamman constructions for effects at 633 and 732 K (Fig. 1c and d) give values of $x = 0.506$ and 0.505, respectively, which are in excellent agreement with the theoretical value of 0.500. A tentative explanation can be given for these two effects: It is very likely that the first of them (at 633 K) corresponds to $RbEuBr_3$ compound formation from Rb_2EuBr_4 and $RbEu_2Br_5$, whereas the second one (at 732 K) is related to the solid–solid transition of this compound. Indeed, the compound's formation at higher temperatures occurs in many LnX_3–MX systems [19, 34, 35, 37] with M = K, Rb or Cs as a "reconstructive phase transition" [37]. Hypothesis about $RbEuBr_3$ compound formation is supported indirectly by exothermic effect observed in DSC curves for the samples with compositions of $0.333 < x < 0.666$. In solid-state reactions which are "reconstructive phase transitions", the arrangement of the ions is drastically changed. Ions have to move from one site to another passing through strong potential walls of other ions. The resulting "kinetic hindrance" can cause great difference between reaction temperatures, measured during DSC heating and cooling runs (thermal hysteresis). In extreme cases of the cooling experiments, the "undercooling" can become so strong that the reaction does not occur in the time-scale of DSC.

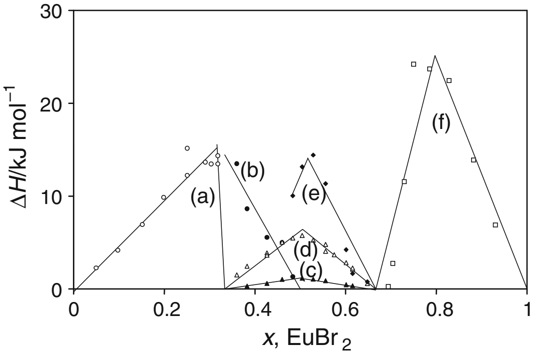

Fig. 1 Tamman diagrams for invariant points in $EuBr_2$–RbBr binary system (detailed description in the text)

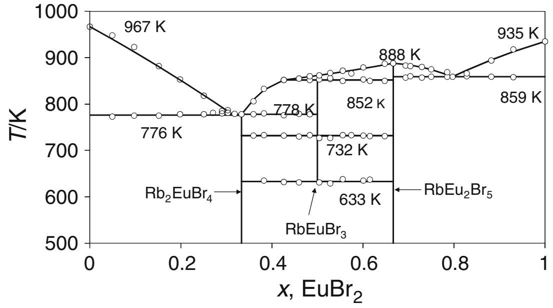

Fig. 2 The $EuBr_2$–RbBr phase diagram

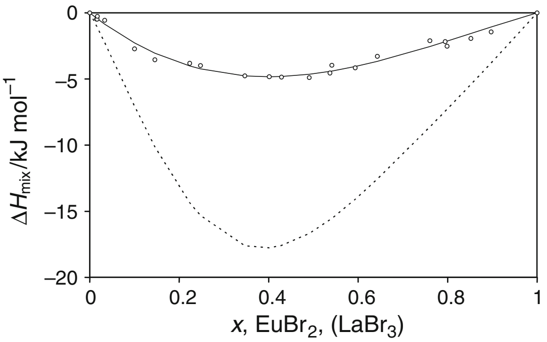

Fig. 3 Molar mixing enthalpy dependence on composition: *open circles* and *solid line*—$EuBr_2$–RbBr, *broken line*—$LaBr_3$–RbBr [39]

Owing to kinetic reasons, the decomposition during cooling takes place no longer, and the compound still exists in the metastable form. Sometimes this "undercooled" decomposition occurs abruptly during subsequent heating run, as it was observed in the case of K_3NdBr_6 [35]. It is very likely that similar situation takes place in the case of $RbEuBr_3$ compound. During cooling, decomposition of this compound is not completed due to kinetic reasons, and some amount of it still exists at room temperature as metastable phase. On the subsequent heating run, this "undercooled" decomposition occurs abruptly, and exothermic effect corresponding to this decomposition appears in the DSC curve. We hope to confirm the above hypothesis by means of X-ray measurements which are planned in the nearest future.

In the composition range of $0.666 < x < 1.0$, only one thermal effect in addition to liquidus (Table 2.) is observed at 859 K (mean value from all the appropriate samples).Taking into account that it disappears at $x = 0.666$ (similarly as the effects related to $RbEuBr_3$), one can expect that $RbEu_2Br_5$ compound also exists in the system. Indeed, this compound exists and melts congruently at 888 K. Accordingly, effect at 859 K corresponds to the $RbEu_2Br_5$–$EuBr_2$ eutectic. The eutectic composition was found from Tamman construction (enthalpy related to the eutectic effect versus composition). The eutectic composition ($x = 0.797$) was determined from the intercept of the two linear parts in Fig. 1f. The enthalpy of fusion of mixture with eutectic composition is equal 25.1 kJ mol^{-1}.

The complete phase diagram is shown in Fig. 2.

Mixing enthalpy

The mixing enthalpy of liquid RbBr–$EuBr_2$ mixtures is negative over the whole composition range (Fig. 3). The minimum of the enthalpy of mixing occurs around the composition $x(EuBr_2) \approx 0.4$. Owing to lack of data, these results could not be compared with mixing enthalpy for the other lanthanide dibromides. The only comparison possible is the comparison with analogous lanthanide tribromide systems. Absolute values of this enthalpy are a few times smaller in comparison with data for trivalent lanthanide bromide–rubidium bromide systems [38–40] (Fig. 3). In general, the enthalpy of mixing in a charge—unsymmetrical mixed cation—common anion systems depends primarily on the charge and size of the two cations and only to a lesser extent on the nature of the common anion. It depends on the "relative ionic potential" of the two cations which can be defined as

$$\Delta IP = \frac{z_1}{r_1} - \frac{z_2}{r_2} \quad (4)$$

where: z_1, z_2, r_1 and r_2 are the valence and the ionic radius of cations, respectively($z_1 > z_2$).The magnitude of the "relative ionic potential" reflects mainly the change in coulombic interaction on mixing, but it is also related to the magnitude of polarization of the common anion by neighboring cations. The larger the "relative ionic potential", the more negative value of the enthalpy of mixing will be (process of mixing is more exothermic). In the case of $LaBr_3$–RbBr mixtures, this "relative ionic potential" is significantly bigger than in the case of $EuBr_2$–RbBr system (2.147 and 1.029 pm^{-1}, respectively, when based on ionic radii given in [41]). Mixing enthalpy is according to this difference and is significantly bigger in

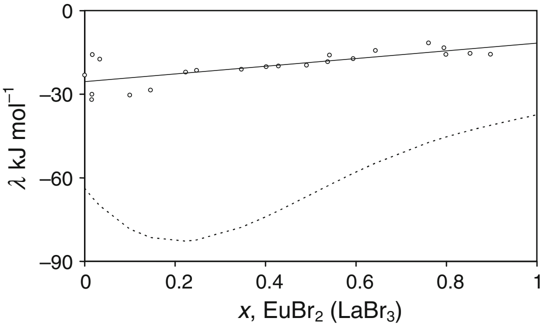

Fig. 4 Interaction parameter λ dependence on composition: *open circles* and *solid line*—$EuBr_2$–RbBr, *broken line*—$LaBr_3$–RbBr [39]

lanthanide (III) bromide systems. Figure 4 shows the composition dependence of the interaction parameter λ

$$\lambda = \frac{\Delta_{\mathrm{mix}} H_m}{x(1-x)} \tag{5}$$

in the melts, together with the same parameter for $LaBr_3$–RbBr melts. The composition dependence of the interaction parameter λ for the $LaBr_3$–RbBr system shows a broad minimum of $x(LaBr_3) \sim 0.25$, which was attributed to the formation of $LaBr_6^{3-}$ complexes in the melts [39]. No minimum was observed on analogical dependence of λ for the system under investigation, mixing enthalpy measurements cannot give information about stoichiometry of complexes formed in these melts. However, the [15] dependence observed earlier of the electrical conductivity of the liquid phase on composition, which shows a broad minimum at $x(EuBr_2) \sim 0.6$, suggests the formation of the complexes in the liquid mixtures. Similarly, the dependence of the activation energy on the changes in conductivity with temperature [15] is indicative of structural changes in melts. The E_A increases up to about 50 mol.% of $EuBr_2$, and becomes almost stable up to 80 mol.% of $EuBr_2$. The stabilization effect on activation energy dependence on composition is very likely the result of different forms of complexes co-existing.

Further structural investigations (neutron diffraction, Raman, and EXAFS) may throw enlightenment on the existence of the complex species in the liquid $EuBr_2$–RbBr binary system.

Conclusions

1. The complete $EuBr_2$–RbBr phase diagram shows that this binary system includes two eutectics and three stoichiometric compounds, namely Rb_2EuBr_4, $RbEuBr_3$ and $RbEu_2Br_5$. The composition and temperature values of eutectics were determined as $x(EuBr_2) = 0.316$; $T_{\mathrm{eut}} = 776$ K, and $x(EuBr_2) = 0.797$; $T_{\mathrm{eut}} = 859$ K. The first compound, Rb_2EuBr_4, decomposes peritectically at 778 K, whereas the second one, $RbEu_2Br_5$, melts congruently at 888 K. The third, $RbEuBr_3$, forms probably at 633 K from Rb_2EuBr_4 and $RbEu_2Br_5$, undergoes the solid–solid phase transition at 732 K and melts incongruently at 852 K.
2. The mixing enthalpy of liquid $EuBr_2$–RbBr mixtures is negative over the whole composition range with minimum at $x(EuBr_2) \sim 0.4$. However, almost linear dependence of interaction parameter λ on composition does not give any information about stoichiometry of the complexes formed in the melts. However, the [15] dependence of the electrical conductivity observed earlier of the liquid phase on composition suggests formation of the complexes in the liquid mixtures.

Acknowledgements L.R, E.I–S and S.G wish to thank the Ecole Polytechnique de Marseille for their hospitality and support during this study.

References

1. Wicks CE, Block FE. Thermodynamic properties of 65 elements—their oxides, halides, carbides and nitrides. U.S. Bureau of Mines Bulletin 605. Washington: U.S. Government Printing Office; 1963.
2. Thoma RE. The rare halides. In: Eyring L, editor. Progress in the science and technology of the rare earths, vol. 2. New York: Pergamon Press; 1966. p. 90–121.
3. Gmelin L. Gmelin handbook of inorganic chemistry. Leipzig: Verlag Chemie g.m.b.H; 1978. pp. 65–76.
4. Nouveau Traité de Chimie Minérale Sous la direction de P. Pascal. Masson et C^{ie} editors, Vol. 7. Paris; 1953. p. 771.
5. Haschke JM, Eick HA. The vaporization thermodynamics of europium dibromide. J Phys Chem. 1970;74:1806–8.
6. YuV Zorenko, Turchlak RM, Gryk W, Grinberg M. Luminescent spectroscopy of Eu^{2+} centers in CsBr: Eu single crystals at 10–550 K. J Lumin. 2004;106:313–20.
7. US Application 20040126489.
8. US Patent 7,038,221.
9. Rycerz L, Gadzuric S, Ingier-Stocka E, Gaune-Escard M. Thermodynamic and structural properties of high temperature solid and liquid $EuBr_2$. J Nucl Mater. 2005;344:115–9.
10. Gadzuric S, Ingier-Stocka E, Rycerz L, Gaune-Escard M. Phase diagram and electrical conductivity of $EuBr_2$–LiBr binary system. J Alloy Comp. 2005;397:63–7.
11. Ingier-Stocka E, Gadzuric S, Rycerz L, Cieslak-Golonka M, Gaune-Escard M. Phase diagram and electrical conductivity of the $EuBr_2$–NaBr binary system. J Nucl Mater. 2005;344:120–3.
12. Rycerz L, Ingier-Stocka E, Cieslak-Golonka M, Wojciechowska A, Gadzuric S, Gaune-Escard M. Physicochemical properties of the $EuBr_2$–KBr binary system. J Alloy Comp. 2008;450:157–61.
13. Gadzuric S. Experimental study of thermodynamic, transport and structural properties of lanthanide bromide systems. Properties prediction by Data Mining Statistical Techniques. Ph. D. Thesis, Universite de Provence, Marseille, France, 2006.
14. Rycerz L, Ingier-Stocka E, Gadzuric S, Gaune-Escard M. Thermodynamic functions of definite compounds formed in $EuBr_2$–MBr binary systems (M = K, Rb). J Chem Eng Data. 2008;53:1266–70.

15. Rycerz L, Ingier-Stocka E, Gadzuric S, Gaune-Escard M. Electrical conductivity of the molten $EuBr_2$–MBr binary mixtures (M = Li, Na, K, Rb, or Cs). J Mol Liq. 2008;140:78–83.
16. Potapov A, Gaune-Escard M. Deviations from the Arrhenius equation of electrical conductivity polytherms. In: Øye HA, Jagtøyen A, editors. Proceedings of international symposium on ionic liquids in honour of professor Marcelle Gaune-Escard. Carry le Rouet, France; 2003, June 26–28. pp. 477–81.
17. Rycerz L, Ingier-Stocka E, Gaune-Escard M. Phase diagram and electrical conductivity of the $CeBr_3$–CsBr binary system. J Thermal Anal Calorim. 2009;97:1015–22.
18. Ingier-Stocka E, Rycerz L, Berkani M, Gaune-Escard M. Thermodynamic and transport properties of the $PrBr_3$–MBr binary systems (M = Li, Na). J Mol Liq. 2009;148:40–4.
19. Rycerz L, Ingier-Stocka E, Gadzuric S, Gaune-Escard M. Phase diagram and electrical conductivity of the $CeBr_3$–RbBr binary system. J Alloy Comp. 2008;450:175–80.
20. Ingier-Stocka E, Rycerz L, Gadzuric S, Gaune-Escard M. Thermal and conductometric studies of the $CeBr_3$–MBr binary systems (M = Li, Na). J Alloy Comp. 2008;450:162–6.
21. Rycerz L, Ingier-Stocka E, Gadzuric S, Gaune-Escard M. Phase diagram and electrical conductivity of $CeBr_3$–KBr. Z Naturforsch. 2007;62a:197–204.
22. Gadzuric S, Ingier-Stocka E, Rycerz L, Gaune-Escard M. Electrical conductivity of molten binary $NdBr_3$–alkali bromide mixtures. Z Naturforsch. 2004;59a:77–83.
23. Ziolek B, Rycerz L, Gadzuric S, Ingier-Stocka E, Gaune-Escard M. Electrical conductivity of molten $LaBr_3$–MBr binary mixtures. Z Naturforsch. 2005;60a:75–80.
24. Delimarskii YUK. Elektrochimiia ionnych rasplavov. Moskva: Mietalurgiia; 1978 (in Russia).
25. Papatheodoru GN, Kleppa OJ. Enthalpies of mixing of liquid nickel(II) chloride-alkali chloride mixtures at 810 °C. J Inorg Nucl Chem. 1970;32:889–900.
26. Papatheodoru GN, Kleppa OJ. Enthalpies of mixing in the liquid mixtures of the alkali chlorides with $MnCl_2$, $FeCl_2$ and $CoCl_2$. J Inorg Nucl Chem. 1971;33:1249–78.
27. Maroni VA, Caims EJ. In: Mamantov G editor. Molten salts. Characterization and analysis. New York, London: Marcel Deker; 1969. p. 231
28. Hayashi H, Uno K, Takechara Z, Katagiri A. Studies on the acid–base properties of the $ZnBr_2$–NaBr molten salt system. J Electrochem Soc. 1993;140:386–9.
29. Adya AK, Takagi R, Gaune-Escard M, Rycerz L, Fischer H. ILL experimental report, experiment N^0 6-03-193. France, Grenoble. 14–22 May 1996
30. Van Artsdalen ER, Yaffe JS. Electrical conductance and density of molten salt systems: KCl–LiCl, KCl–NaCl and KCl–KI. J Phys Chem. 1955;59:118–27.
31. Yaffe JS, van Artsdalen ER. Electrical conductance and density of pure moltenalkali halides. J Phys Chem. 1956;60:1125–31.
32. Haschke JM, Eick HA. The preparation and some properties of europium bromides and hydrated bromides. J Inorg Nucl Chem. 1970;32:2153–8.
33. Gaune-Escard M, Bogacz A, Rycerz L, Szczepaniak W. Heat capacity of $LaCl_3$, $CeCl_3$, $PrCl_3$, $NdCl_3$, $GdCl_3$, $DyCl_3$. J Alloy Comp. 1996;235:176–81.
34. Rycerz L. High temperature characterization of LnX_3 and LnX_3–AX solid and liquid systems (Ln = Lanthanide, A = Alkali, X = Halide): thermodynamics and electrical conductivity. Ph. D. Thesis, Marseille; 2003.
35. Rycerz L. Thermochemistry of lanthanide halides and compounds formed in lanthanide halide-alkali metal halide systems (in Polish). Scientific papers of institute of inorganic chemistry and metallurgy of rare elements. Wroclaw University of Technology, Series Monographs 35, Wroclaw; 2004.
36. Gaune-Escard M. In: Gale R, Lovering DG editors. Molten salt techniques, Chapt. 5. New York, London: Plenum Press; 1991.
37. Seifert HJ. Ternary chlorides of the trivalent early lanthanides. Phase diagrams, crystal structures and thermodynamic properties. J Thermal Anal Calorim. 2002;67:789–826.
38. Gaune-Escard M, Bogacz A, Rycerz L, Szczepaniak W. Calorimetric investigations of the MBr–$NdBr_3$ melts (M = Li, Na, K, Cs). J Thermal Anal. 1995;45:1117–24.
39. Gaune-Escard M, Bogacz A, Rycerz L, Szczepaniak W. Formation enthalpies of the MBr–$LaBr_3$ liquid mixtures (M = Li, Na, K, Rb, Cs). Thermochim Acta. 1996;279:1–10.
40. Gaune-Escard M, Bogacz A, Rycerz L, Szczepaniak W. Formation enthalpies of the MBr–$NdBr_3$ liquid mixtures (M = Li, Na, K, Rb, Cs). Thermochim Acta. 1996;279:11–25.
41. Sharpe G. Inorganic chemistry. New York: Longman; 1986. p. 146 and 659.